

Are carbon deflagration supernovae triggered by dark matter ?

JEREMY MOULD^{1,2}

¹*Swinburne University*

²*ARC Centre of Excellence for Dark Matter Particle Physics*

ABSTRACT

Collisions between stellar remnants and dark matter in the Galactic bulge are frequent, and the kinetic energy of a primordial black hole incident on a white dwarf, if it is all thermalized, will raise the degenerate core's temperature, by at least a degree in the case of a lunar mass black hole. This is an underestimate in two ways: the specific heat is less than $3k/2$ per particle, and the incoming object is accelerated by gravitational focusing. Detailed physical models have recently been made of this triggering event. Present observational data are equivocal as to whether the radial distribution of type Ia supernovae in galaxies follows the starlight in the galaxies, or is more concentrated towards the center, as collisional triggering would suggest. But future samples of millions of supernovae from the Rubin telescope will change that.

Keywords: Type Ia supernovae 1728 – White dwarfs 1799 –Dark matter 353 – primordial black holes

1. INTRODUCTION

Carbon deflagration supernovae (SNe) are one of the best predictions of stellar astrophysics. They are also a pillar of observational cosmology. But does the degenerate core of the Chandrasekhar mass white dwarf spontaneously explode, or is it triggered ? This question is almost as old as electron degeneracy, but simulations of a triggering process have recently caught up (Leung et al. 2025). Earlier work is by Graham et al. (2015). In this paper we examine the observational evidence that exists for dark matter (DM) triggering of SNeIa. If triggering by primordial black holes (PBHs) occurs, the best place to look for SNeIa would be the centers of galaxies, where the peak density of DM is found. We also investigate the number density squared rate dependence of dark matter triggering in galaxies from the Millennium simulation.

2. OBSERVATIONS

The Dark Energy Survey (DES, Troxel et al. 2017) and OzDES³ recorded and measured redshifts for 1829 type Ia SNe. Toy et al. (2023), using a redshift independent measure of radial distance of the SN distance from the center of each galaxy, published the data in Figure 1. This measure is also independent of surface brightness dimming (see Appendix).

To compare this with expectations from theory we need to relate the radial quantity d_{DLR} with the exponential disk (Freeman 1970) of spiral galaxies and the $r^{1/4}$ law of ellipticals (de Vaucouleurs 1959). The quantity d_{DLR} is the second moment of the radial distribution, and for exponential disks this is $2a^2 - a$ for disk scale radius a . Therefore $4d_{DLR} = 1 + \sqrt{8a}$. If the radial SN distribution follows the light of the old stellar population, then the green curve is the expectation. For the $r^{1/4}$ law, numerical integration is required to obtain the second moment, and the result is the blue curve in Figure 1.

In a galaxy with white dwarf number density n_* and dark matter number density n_\bullet , the rate per unit volume of collisions is $n_* n_\bullet \sigma v$, where σ is the collision cross section and v is the relative velocity. For spontaneous deflagration the same rate is just n_* .

³ <http://mso.anu.edu.au/ozdes>

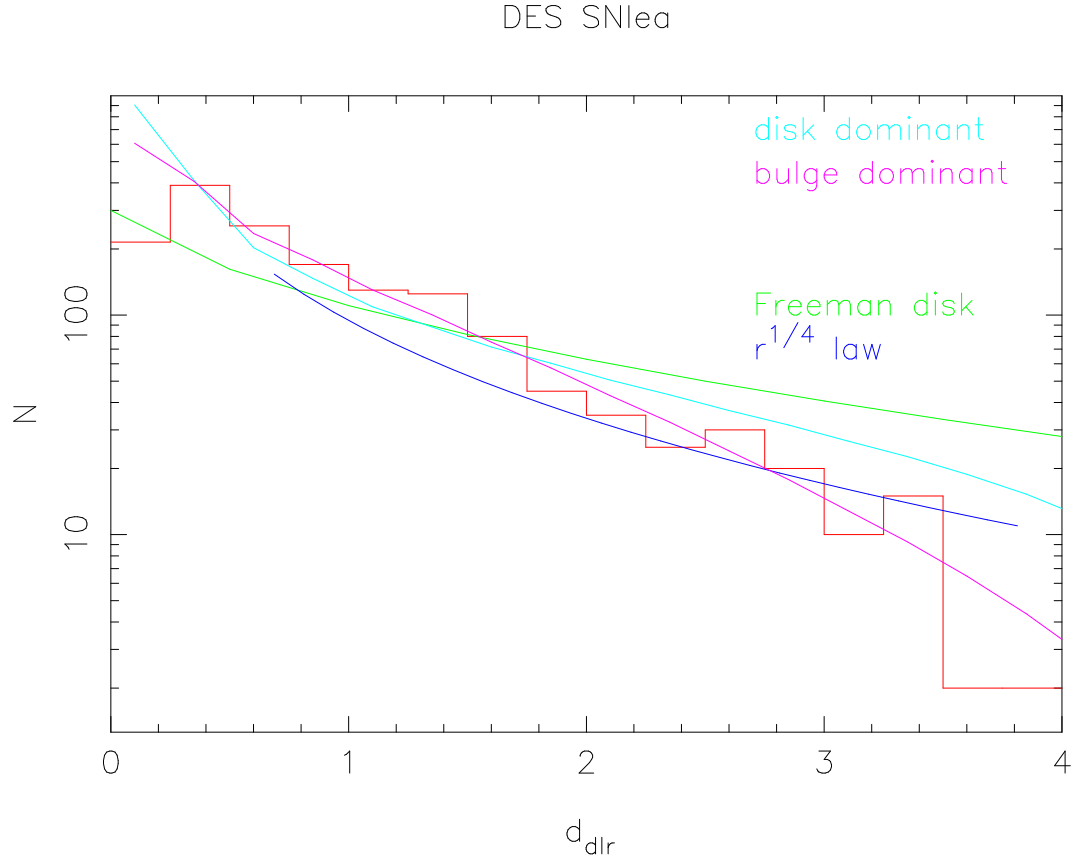


Figure 1. Radial distribution of SNeIa in the Dark Energy Survey (in red). The green curve is the expectation for exponential disks and the blue curve for elliptical galaxies. These have not been normalised to the data. The other two curves are for DM triggered SNe, and these have been normalized to the same total number of SNe, excluding the first, central bin, which is anomalous, and is conceivably a selection effect of some SN being masked by the nucleus.

Table 1. Galactic bulge contents

Species	BH	NS	WD	MS
Initial Mass	max, min	min	min	min
M_{\odot}	100, 3.5	1.17	0.7	0.1
$\int n(m) m dm$	$\log(100/3.5)$	$\log(3.5/1.17)$	$\log(1.17/0.7)$	$\log(7)$
Mass $10^{10} M_{\odot}$	$1.60/3$	$0.52/3$	$0.25/3$	$0.93/3$
$\int n(m) dm$	$3.5^{-1}-0.01$	$1.17^{-1}-3.5^{-1}$	$1.43-1.17^{-1}$	$10-0.7^{-1}$
$N 10^{10}$	$0.28/3$	$0.57/3$	$0.58/3$	$8.57/3$

MS = main sequence, NS = neutron star

3. TRIGGERED SUPERNOVA RATES

The Galactic bulge is the densest region of our Galaxy, and so the most favorable for high collision induced SN rates. The make-up of the Galactic bulge, an old stellar population, is given in Table 1 for an initial mass function $n(m) \propto m^{-2}$, close to the Salpeter function. The mass of the bulge $1.1 \times 10^{10} M_{\odot}$ is taken from Binney & Vasiliev (2023). The rate per unit volume of collisions between these objects is

$$\rho = n_1 n_2 \sigma v \quad (1)$$

where σ is the cross section, v is the velocity, V is the volume and n_1, n_2 are the number densities of the interacting objects. Gravitational focussing increases the probability of collision by a factor⁴ of $g = (1 + v_{esc}^2/v^2)$ (Barnes 2011, Seligman, Marceta, & Peña-Asensio 2026), where $v_{esc}^2 = 2 G (M_1 + M_2)/(R_1 + R_2)$. The small denominator of g yields a value of 4.8×10^5 .

If PBHs are a fraction f of the Galaxy's dark matter and a density of 0.01 to 0.1 $M_\odot \text{ pc}^{-3}$ can be assumed for the Galaxy's dark matter core (Cole & Binney 2016, Lazar et al. 2020), then for a lunar mass PBH ($10^{-7} M_\odot$) equation 1 gives a rate of 12.6 to 126 $fv = 13.8 \text{ to } 138 f \sqrt{3} \times 10^2 \text{ Myr}^{-1}$ for a 1D DM velocity dispersion of 110 km s^{-1} . The density of L^* galaxies (like the Milky Way) is approximately (Blanton et al. 2003, Bell et al. 2003) $0.01 h^3 \times \text{Mpc}^{-3} = 3.9 \times 10^6 \text{ Gpc}^{-3}$ for $h = 0.73$ (Riess et al. 2024). Over a cosmic volume this rate becomes 0.9 to 9 $f \times 10^4 \text{ Gpc}^{-3} \text{ yr}^{-1}$, compared with the observed rate of $(2.55 \pm 0.12) \times 10^4 \text{ yr}^{-1} \text{ Gpc}^{-3} h_{70}^3$ (Desai et al. 2026). For $f \sim 20\%$ of the dark matter this is consistent with the rate estimate from observation. This value is close to upper limits from microlensing observations. Two other parameters need mentioning. Leung et al. (2026) ran white dwarf models down to $0.7 M_\odot$. Our triggered SN rate would reduce by an eighth if the $0.7\text{--}0.8 M_\odot$ failed to explode or burn. And sub-lunar mass PBHs would produce more SNeIa, and that can be compensated by reducing the parameter f , the fraction of the DM in PBHs.

To calculate the radial distribution of SNeIa triggered by PBH collisions, one can assume the NFW profile for the DM and use the following quantities provided for the Millennium simulation Springel et al. 2005) by the Theoretical Astrophysical Observatory (TAO: Bernyk et al. 2016): Stellar mass, bulge mass, DM halo mass, disk scale radius, and virial radius. The surface density of SNeIa is then the integral of the volume density along the line of sight through the galaxy.

$$n(r) = \int \rho(s) dr' \quad (2)$$

where $s = \sqrt{(r^2 + r'^2)}$. The ratio of the virial radius to the scale radius in the NFW profile was assumed to be 12.

The acceptance criterion for TAO galaxies was stellar mass $10^9 < \text{stellar mass} < 10^{10.5}$ and satellite galaxies were rejected. Of these, every fifth galaxy was selected, and 8811 disk dominated galaxies were chosen (disk mass $>$ bulge mass) and 2146 bulge dominated galaxies. The results were averaged and plotted as labeled in Figure 1. There is considerable variance between galaxies, but the statistics have shrunk the error bars to about the width of the plotted curves. By eye, only the pure (untriggered SN) Freeman disk is a poor fit.

4. HISTORICAL SUPERNOVAE

Supernovae since 1930 have been recorded by the Central Bureau for Astronomical Telegrams⁵ and it was possible⁶ to download those before 2015. The offset of the SN from the center of the galaxy is frequently recorded in arcsec. These can be made distance independent by dividing by the D_{25} diameter, available in many cases from the NED database. For a Freeman disk the relationship is $a = D_{25}/6.8 \times 2.5/\ln(10)$. The values of D_{25} are subject to $(1+z)^4$ surface brightness dimming with redshift z . I correct for this by dividing the diameters by $(3.4-10z)/3.4$, the numerical value 3.4 being the difference between the central surface brightness of the disk, 21.6 B mags per arcsec², and the 25th mag isophote. For the historical SNe at low z this is a small correction, as shown in Figure 2 (upper left). Figure 2 shows that such a disk is a good fit to the radial distribution, with no sign of the excess central concentration seen in Figure 1.

The lower two panels of Figure 2 show galaxies with K band 2MASS isophotal diameters. Their correction for surface brightness dimming and their transformation to D_{25} by dividing by 0.69 is indicated in the Appendix. The historical SNe do not support the higher central concentration seen in the DES SNe. No correction has been made for selection effects in either survey, and this is an area where future work can improve confidence in the results. Table 2 contains host galaxies indicated as anonymous by CBAT which were linked with their SNeIa by NED using a radius of $0.18'$. The column labeled 2MASS lists their 2MASS isophotal diameters.

5. THE RUBIN OBSERVATORY

This is an exceptionally well suited problem for Rubin telescope surveys to solve. Images of every recorded SN and the surface brightness profile of its host galaxy provide all the data needed to repeat the work outlined here with

⁴ Naïvely, this factor can be seen as the ratio of solid angles of the two velocity ellipsoids

⁵ <http://www.cbat.eps.harvard.edu>

⁶ More recent SNe are available by subscription.

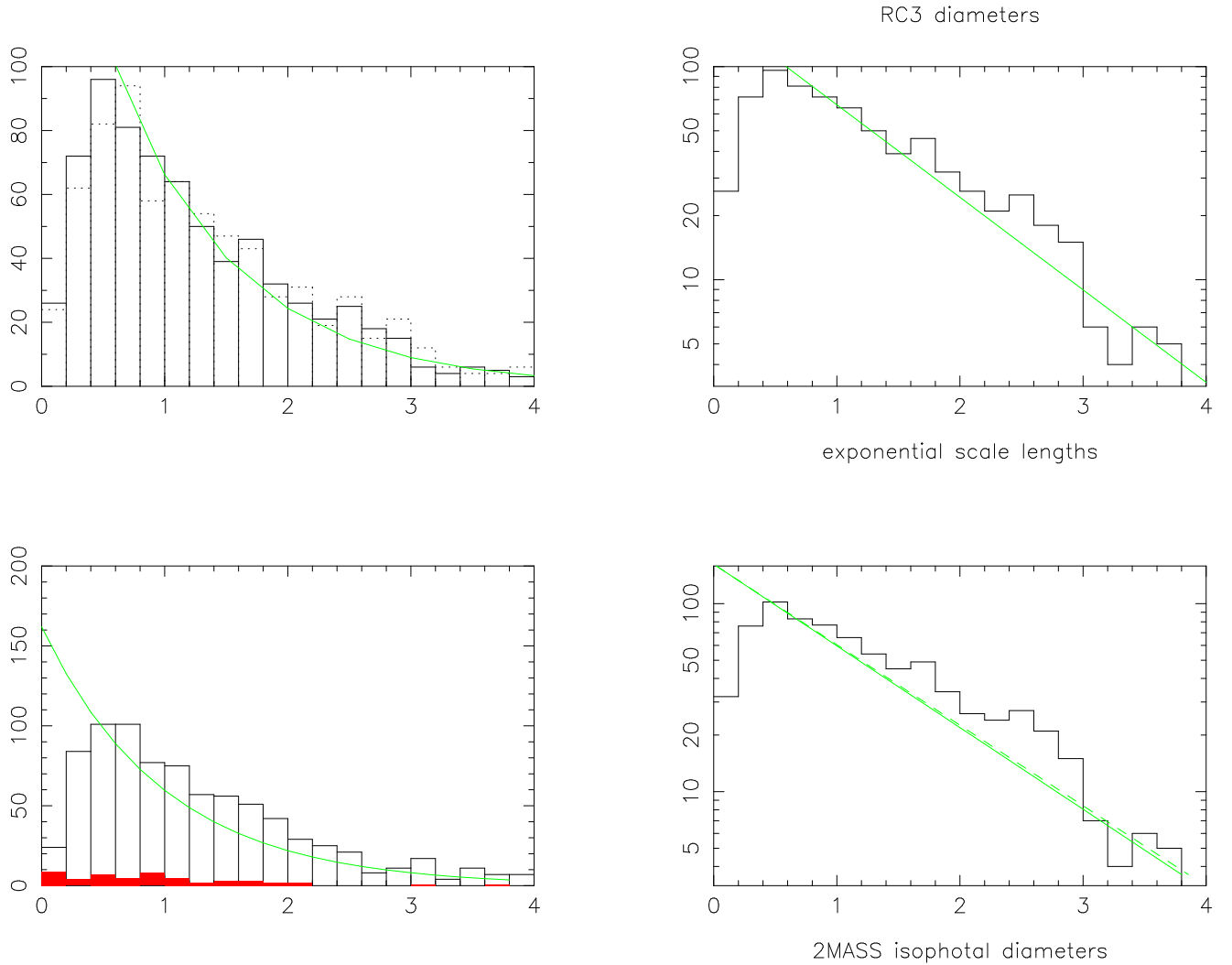


Figure 2. The top two panels are the radial distribution of SNeIa scaled to remove distance dependence as described in the text, using the RC3 diameter D_{25} (de Vaucouleurs et al. 1976). The solid histogram (upper left) has been corrected for $(1+z)^4$ surface brightness dimming, and the dotted histogram has not. The difference is small for these low z galaxies. The lower two panels use the total magnitude K band radius from the 2MASS survey. The shaded red histogram is the galaxies in Table 2 shown separately. In the bottom right hand plot they have been added in. In general the slope of these histograms is shallower than the expectation from the stellar light (the green curves and lines).

definitive effect. This may permit issues with galaxy surface brightness fitting to be avoided. Note that it is the surface brightness of the old stellar population that is relevant to these SNeIa, and that §3 showed that the central density of the DM is the largest uncertainty in any rate prediction for triggered SNe. Key data to be recorded are the surface brightness of the position of the SN in the post-SN galaxy, the SN type and the galaxy redshift. Selection effects masking nuclear SNeIa need to be carefully modeled.

ACKNOWLEDGEMENTS

My thanks to Xiuqin Wu for advice on the NED queries in §4 and to Darren Croton for help with TAO. This research has made use of the NASA/IPAC Extragalactic Database (NED) which is operated by the California Institute

of Technology, under contract with NASA Award Number 80NSSC21M0037⁷. The Central Bureau for Astronomical Telegrams and the Minor Planet Center are services of the International Astronomical Union and operated by Dept. of Earth and Planetary Sciences, Harvard University. The 2MASS project is a collaboration between The University of Massachusetts and the Infrared Processing and Analysis Center (JPL/ Caltech). Funding was provided primarily by NASA and the NSF. TAO is part of the All-Sky Virtual Observatory (ASVO) and is funded and supported by Astronomy Australia Limited, Swinburne University of Technology and the Australian Government. The latter is provided through the Commonwealth's Education Investment Fund and National Collaborative Research Infrastructure Strategy.

REFERENCES

Barnes, R. 2001, "Gravitational Focusing", in Gargaud, Amils, Quintanilla, Cernicharo, & Henderson eds., Encyclopedia of Astrobiology, Berlin, Heidelberg: Springer, p. 692

Bell E. F., McIntosh D. H., Katz N., Weinberg M. D., 2003, ApJS, 149, 289

Blanton M. R. et al. 2003, ApJ, 592, 819

Bernyk, M. et al. 2016, ApJS, 223,9

Binney, J. & Vasiliev, E. 2023, MNRAS, 520, 1832

Cole, D. & Binney, J. 2016, MNRAS, 465, 798

Croton, D. et al. 2023, <http://dx.doi.org/10.26185/642bbd010a9ca>

de Vaucouleurs, G. 1959, Handbuch der Physik (Springer-Verlag, Berlin, Göttingen), Vol. 53.

de Vaucouleurs, G., de Vaucouleurs, A. & Corwin 1976, Reference Catalog of Bright Galaxies

Desai, D., Shappee, B. Kochanek, C. et al. 2026, arXiv 2602.00223

Freeman, K. 1970, ApJ, 160, 811

Graham, P., Rajendran, S. & Varela, J. 2015, PhRvD, 92f3007

Lazar, A. et al. 2020, MNRAS, 497, 2393

Leung, Shing-Chi, Walther, S., Nomoto, K. & Kusenko, A. 2025, ApJ, 991, 11

Riess, A. et al. 2024, ApJ, 977, 120

Seligman, D., Marceta, D. & Peña-Asensio, E. 2026, ApJ, 997, 146

Springel V. et al. 2005, Nature, 435, 629

Toy, M. et al. 2023, MNRAS, 526, 5292

Troxel, M. et al. 2018, PhRvD, 98d3528

APPENDIX

To compare 2MASS isophotal diameters with RC3 D_{25} diameters we show the ratio in Figure A1 for those galaxies that have both. The mean value and the median are 0.690 ± 0.008 .

Surface brightness dimming affects galaxy diameter measurements. In magnitudes the effect is $2.5\log(1+z)^4 = 10\log(1+z)$, where z is the redshift. A value of D_{25} can be corrected by multiplying by $3.4/(3.4-10z)$ for $z << 1$, 3.4 being the difference between the 25th mag isophote and the central surface brightness of a Freeman disk: 21.6 mag arcsec $^{-2}$. In Figure A2 we show the effect on the highest redshift sample, which is Table 2. The correction factor was $2.346/(2.346-10z)$ for $z << 1$.

Table 2. Deanonymized galaxies from CBAT

SN	r arcsec	Host	2MASS	cz
			arcsec	km s ⁻¹
6	2015ax	12.2	WISEAJ011814.92+150556.7	20.8
	2014ci	4.5	WISEAJ223404.03+682630.3	78.6
	2014ch	1.4	WISEAJ155830.83+125155.3	15.4
	2014am	6.1	WISEAJ152318.43+181728.1	17.4
	2013ew	32.0	WISEAJ221009.32+111657.1	27.0
	2012da	22.8	WISEAJ130233.83+272610.4	22.2
	2012ae	3.2	WISEAJ085856.06+230341.0	21.0
	2011hz	1.0	WISEAJ085234.32+551513.5	11.4
	2010lk	2.2	WISEAJ091514.39+012213.4	52.4
	2010ix	14.6	WISEAJ010002.74+414306.5	25.6
	2009mp	0.0	WISEAJ092359.89+140646.9	23.0
	2009jm	1.0	WISEAJ225014.07+103333.8	20.4
	2009hw	2.2	WISEAJ192033.98+433349.2	13.6
	2009ez	0.0	WISEAJ131254.43+432836.0	13.8
	2009eg	7.1	WISEAJ145415.48+185746.7	13.6
	2009df	0.0	WISEAJ160553.08+172438.8	10.0
	2009co	6.1	WISEAJ122435.85+471415.2	12.2
	2009cm	0.0	WISEAJ115442.17+551810.6	10.0
	2009aw	6.4	WISEAJ063146.75+245509.5	13.0
	2006eq	9.9	WISEAJ212837.50+011346.3	16.2
	2006da	4.5	WISEAJ232748.75+142831.1	20.6
	2006ct	3.2	WISEAJ120956.71+470545.5	14.2
	2006cj	4.5	WISEAJ125924.11+282049.8	14.2
	2006cg	3.6	WISEAJ130502.54+284420.4	25.2
	2005hf	2.8	WISEAJ012705.85+190701.8	19.8
	2005eu	1.4	WISEAJ022743.32+281037.7	24.2
	2005be	7.1	WISEAJ145933.08+164006.8	17.6
	2003hw	3.6	WISEAJ030149.87+354435.2	22.6
	2003ay	7.3	WISEAJ040726.44+280748.4	12.8
	2003av	4.1	WISEAJ080132.37+024825.9	11.6
	2002eu	15.6	WISEAJ014943.12+323736.3	124.8
	2002lq	4.1	WISEAJ164028.34+411409.7	26.0
	2001bp	7.2	WISEAJ160208.91+364313.9	14.2
	1999ax	3.6	WISEAJ140357.57+155111.7	21.2
	1998aa	10.0	WISEAJ122532.63+073859.6	21.8
	1997ea	9.5	WISEAJ074836.75+521319.9	24.0
	1996bl	6.7	WISEAJ003617.70+112342.6	24.8
	2000fs	0.0	NGC 1218	84.8
	2014ap	8.6	CGCG 126-07	39.0
	2013fj	5.8	CGCG 428-06	21.8
	2013ey	3.6	CGCG 425-02	26.8
	2012eo	9.2	CGCG 494-00	32.8
	2012dg	10.0	CGCG 254-03	30.4
	2010ew	8.6	CGCG 173-01	20.2
	2006te	6.3	CGCG 207-04	27.0
	2005bu	8.1	CGCG 117-01	29.2
	2004ck	10.6	CGCG 064-09	20.2
	2002bf	4.1	CGCG 266-03	38.6
	2002aw	2.8	CGCG 189-02	32.0
	2000fo	8.5	CGCG 475-01	39.4
	2000df	9.5	CGCG 051-07	24.4
	2000cv	10.0	CGCG 292-08	22.8
	1996ac	3.6	CGCG 014-02	21.8
	SN2014K	7.1	CGCG 332-20	22.4
	SN2012B	9.4	CGCG 526-10	24.2
	SN2010V	7.8	CGCG 163-59	34.2
	SN1999X	7.2	CGCG 180-22	28.8
	SN1994Q	4.0	CGCG 224-10	21.2

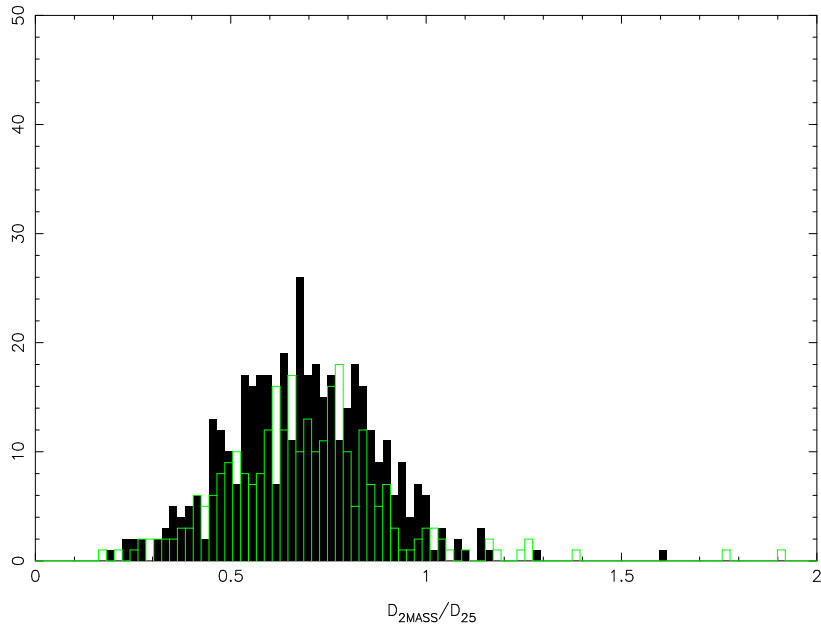


Figure A1. Ratio of 2MASS isophotal diameters to RC3 D_{25} diameters. There is no noticeable difference between the black $z < 0.02$ subsample and the green $z > 0.02$ one.

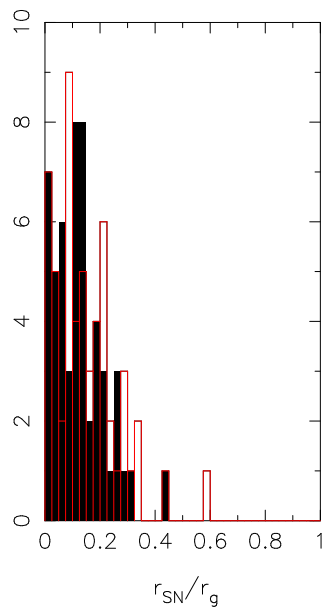


Figure A2. Raw SN radii divided by 2MASS radius (red histogram). The solid black histogram has been corrected for surface brightness dimming.